

## Hollow Chitosan/Poly(acrylic acid) Nanospheres as Drug Carriers

Yong Hu,<sup>†</sup> Yin Ding,<sup>‡</sup> Dan Ding,<sup>‡</sup> Mingjie Sun,<sup>§</sup> Leyang Zhang,<sup>‡</sup> Xiquan Jiang,<sup>\*,†,||</sup> and Changzheng Yang<sup>‡</sup>

National Laboratory of Solid State Microstructure, Department of Material Science and Engineering, Nanjing University, Nanjing, 210093, P. R. China, Laboratory of Mesoscopic Chemistry and Department of Polymer Science & Engineering, College of Chemistry & Chemical Engineering, Nanjing University, Nanjing, 210093, P. R. China, Department of Biochemistry, Nanjing University, Nanjing, 210093, P. R. China, and Jiangsu Provincial Laboratory for Nanotechnology, Nanjing University, Nanjing, 210093, P. R. China

Received August 23, 2006; Revised Manuscript Received December 22, 2006

The preparation, in-vitro release, in-vitro cytotoxicity, and in-vivo drug delivery of doxorubicin (DOX)-loaded chitosan (CS)-poly(acrylic acid) (PAA) hollow nanospheres were investigated. The loading was done by dissolving a certain amount of DOX in non-cross-linked CS-PAA nanospheres aqueous solution followed by cross-linking chitosan with glutaraldehyde. The drug-loading content was up to 4.3% and the size of drug-loaded hollow nanospheres, determined by dynamic light scattering, was 118 nm. The nanospheres showed a continuous release of the entrapped DOX up to 10 days in vitro and showed comparable in-vitro cytotoxicity against HepG2 cells compared to the free DOX. In-vivo DOX delivery of DOX-loaded CS-PAA nanospheres showed that DOX concentration in blood can be maintained for a longer period than free DOX solution, and the DOX concentration in mice liver can be maintained constantly at relatively high level. The interesting feature of DOX-loaded CS-PAA hollow nanospheres is that the loaded DOX can be delivered into the mice brain. The confocal laser scanning microscopy analysis reveals that fluorescein isothiocyanate (FITC)-labeled CS-PAA can deposit in different organs including liver, spleen, and brain.

### Introduction

Recently, biocompatible polymeric nanoparticles have been extensively investigated for both therapeutic (e.g., drug delivery) and diagnostic (e.g., imaging) purposes.<sup>1–4</sup> As a successful drug delivery vehicle, polymeric nanoparticles should have the ability to deliver drug to desirable sites and to escape from the biological particulate filter known as the reticuloendothelial system (RES), resulting in long circulating in vivo.<sup>5</sup> On the basis of these considerations, many types of nanosized polymeric carriers were developed, including polymeric micelles,<sup>6</sup> polymer-modified liposome,<sup>7</sup> and some other colloidal systems.<sup>8</sup> Among them, hollow polymeric nanospheres have received increasing attention because they have the potential ability to encapsulate large quantities of guest molecules or large-sized functional materials within their empty core domain. So far, many methods have been developed to construct hollow micro- or submicro-spheres including layer-by-layer (LBL) deposition of polyelectrolytes on a template core,<sup>9</sup> polymerizing monomer on a liquid core,<sup>10</sup> and pH induced micellization of a grafted polymer.<sup>11</sup> Although these methods are quite successful and have been applied in an extended field, rather limited work has been reported on their application in drug delivery because most of hollow spheres described to date are composed neither of biocompatible nor of biodegradable materials.

Chitosan (CS) is a biodegradable polysaccharide extracted from crustacean shells. Because of its good biocompatible, biodegradable, and low toxic properties, chitosan has been widely used in biomedical field as a carrier for drugs or other biomaterials.<sup>12</sup> Chitosan is also a cationic polyelectrolyte and can form nanoparticles with an anionic polyelectrolyte, such as tripolyphosphate (TPP),<sup>13</sup> dextran sulfate,<sup>14</sup> alginate,<sup>15</sup> and plasmid.<sup>12</sup> To prepare CS-based hollow spheres, our group recently developed a method for the preparation of hollow nanospheres and hollow composite nanospheres of chitosan/poly(acrylic acid) in aqueous solution on the basis of the polymerization of acrylic acid inside chitosan–acrylic acid micelles and demonstrated that this is a simple and direct method to fabricate hollow polymeric nanospheres with biocompatible and biodegradable materials.<sup>16–18</sup>

Doxorubicin (DOX) is an anticancer agent of broad spectrum with reasonable therapeutic index and intriguing biological and physicochemical actions.<sup>19</sup> However, DOX also has a strong cytotoxic action to normal tissues and produces extensive biochemical effects on the body. To decrease the toxic side effects of DOX, loading doxorubicin to nanoparticles is a promising solution.<sup>20–22</sup>

In this work, we report the investigation of hollow CS-PAA nanospheres as the drug carrier and their drug release pattern in vitro and in vivo with DOX as a model drug. As we previously reported that the PAA was localized in the inner shell of the CS-PAA hollow nanosphere,<sup>18</sup> we expected that DOX containing an amino group could penetrate into the CS-PAA hollow nanospheres and complex with PAA component to improve the drug encapsulation efficiency. Further, the cytotoxicity of DOX loaded CS-PAA hollow nanospheres in cell line and its biodistribution in vivo were investigated.

\* To whom correspondence should be addressed. Fax: 86-25-83317761; e-mail: jiangx@nju.edu.cn.

<sup>†</sup> Department of Material Science and Engineering.

<sup>‡</sup> College of Chemistry & Chemical Engineering.

<sup>§</sup> Department of Biochemistry.

<sup>||</sup> Jiangsu Provincial Laboratory for Nanotechnology.

## Experimental Section

**Materials.** Chitosan (CS) (Nantong Shuanglin Biological Product Inc.) was refined twice as following. First, chitosan was dissolved in dilute acetic acid solution and the solution was filtered. Then, the filter liquor was poured into aqueous NaOH solution to precipitate CS and the precipitated CS was washed with distilled water. Finally, the CS was dried in a vacuum at room temperature for use. The deacetylation degree of CS was 88%, and the average molecular weight of chitosan was 200 kDa determined by viscometric methods.<sup>23</sup> Potassium persulfate ( $K_2S_2O_8$ ) was recrystallized from distilled water. Acrylic acid (AA) (Shanghai Guanghua Chemical Company) was distilled under reduced pressure in nitrogen atmosphere. Doxorubicin hydrochloride was obtained as a gift from Shenzhen Main Luck Pharmaceuticals Inc. (Shenzhen China) in powder. 3-(4,5-Dimethylthiazol-2-yl)-2,5-diphenyltetrazolium bromide (MTT) was purchased from BDH Laboratory Supplies (Poole, Dorset, England). Fluorescein isothiocyanate (FITC) and glutaraldehyde (GA) were purchased from Sigma Chemical Company (St. Louis, MO). Jung tissue freezing medium was purchased from Leica, United States. All other reagents were of analytical grade and were used without further purification except methanol used for high-performance liquid chromatography (HPLC).

**Preparation of DOX-Loaded CS-PAA Hollow Nanospheres.** According to our previous report,<sup>18</sup> CS-PAA hollow nanospheres were first prepared. Briefly, 0.5 g of purified CS was dissolved in 50 mL AA solution with predetermined acrylic acid amount under magnetic stirring. Until the solution became clear, the desired amount of  $K_2S_2O_8$  was added to the solution with continuous stirring. Then, the polymerization was carried out at 70 °C under a nitrogen stream and magnetic stirring. The polymerization was completed in 2 h and got an opalescent suspension. The sample was filtered with the paper filter to remove polymer aggregates. The residual AA monomers in suspension were removed by dialysis in a buffer solution of pH = 4.5 for 24 h using a dialysis membrane bag (12 kDa cut off). After this, a determined amount of glutaraldehyde (glucosamine unit in CS:aldehyde unit in GA = 1.1:1) was added to this system which continued to react for 2 h at 40 °C. These non-drug-loaded hollow nanospheres were abbreviated as CS-PAA or called empty CS-PAA nanospheres.

Drug-loaded hollow nanospheres were got by dissolving a certain amount of DOX in 50 mL acquired nanospheres suspension before GA was added into this system. When DOX was incubated in this system for 48 h, GA was added and reacted as described above. Finally, the drug-loaded nanospheres were separated from the aqueous solution by centrifugation (Ultra ProTM 80, DuPont) at 8000 r/min and 4 °C for 15 min. The resulting drug-loaded CS-PAA nanospheres were abbreviated as CS-PAA-DOX and were kept in the wet state.

**Fluorescence-Labeled CS-PAA Hollow Nanospheres.** FITC-labeled CS-PAA hollow nanospheres were prepared as reported with some modification.<sup>24</sup> Five milliliters of methanol with 2.0 mg/mL FITC solution was added into 50 mL prepared CS-PAA hollow nanospheres solution, and the mixture was stirred at room temperature for 24 h in the dark. Then, these FITC-labeled CS-PAA nanospheres were separated by centrifugation at 4 °C. The obtained sediment was washed and redispersed in the mixture of methanol and distilled water (1:9 v/v) three times to removed the unreacted FITC. Finally, the obtained FITC-labeled CS-PAA nanospheres were dispersed in aqueous solution with a pH value of 5.0 for the in-vivo experiment.

**Fourier Transform Infrared (FT-IR) Measurement of Hollow Nanospheres.** FT-IR spectra were recorded by a Bruker IFS66V vacuum-type spectrometer to determine the chemical structure of these nanospheres. The CS-PAA nanospheres and CS-PAA-DOX nanospheres, which were purified by centrifugation separation, were lyophilized to dry powder and were measured in KBr pellet.

**Size and Zeta Potential Analysis of Hollow Nanospheres.** Mean diameter and size distribution of the prepared DOX-loaded and blank CS-PAA nanospheres were determined by dynamic light scattering

(DLS) method using a Brookhaven BI 9000AT system (Brookhaven Instruments Corporation, United States). Zeta potential of the nanospheres was obtained with Zetaplus (Brookhaven Instruments Corporation, United States). Each sample of the nanospheres was adjusted to a concentration of 0.01% (wt/v) in filtered distilled water or in 0.1 mol/L NaCl solution in the case of zeta potential examination. All analyses were triplicate and the results were the average of three runs. All DLS measurements were done with a laser wavelength of 658.0 nm at 25 °C.

**DOX Encapsulation Efficiency.** Encapsulation efficiency (EE) and DOX loading content (LC) in the nanospheres were determined by centrifugation method. The CS-PAA-DOX nanospheres were separated from the aqueous suspension medium by centrifugation at 40 000 r/min for 40 min at 4 °C. The obtained pellet was incubated at 60 °C in vacuum state overnight and was weighted. DOX concentration in supernatant was analyzed by the ultraviolet absorption (UV) at the wavelength of 480 nm, a strong absorption band of DOX, with reference to a calibration curve on a Shimadzu UV3100 spectrophotometer (Shimadzu, Japan). The measurements were performed in triplicate. The amount of the drug in the nanospheres could be calculated by addition amount of DOX subtracting DOX one in supernatant. Drug-loading content and encapsulation efficiency were obtained by eqs 1 and 2, respectively.

$$\text{drug-loading content \%} = \frac{\text{weight of the drug in nanoparticles}}{\text{weight of the nanoparticles}} \times 100\% \quad (1)$$

$$\text{encapsulation efficiency \%} = \frac{\text{weight of the drug in nanoparticles}}{\text{weight of the feeding drug}} \times 100\% \quad (2)$$

where the weight of the feeding drug which represents the total amount of doxorubicin that was added into the system

**Drug Release from the CS-PAA-DOX Hollow Nanospheres in Vitro.** One hundred milligrams of DOX loaded CS-PAA nanospheres was resuspended in 10 mL saline solution (0.9% NaCl, wt/wt) and was placed in a dialysis membrane bag (12 kDa cut off), was tied, and was sank into 300 mL of saline. The entire system was kept at 37 °C with continuously magnetic stirring. After a predetermined period, 5 mL of the saline medium was drawn out from release system for analysis, and 5 mL of fresh medium was added into the release system. The released DOX amount was determined by UV analysis with a calibration curve as described above.

**Cytotoxicity Assay.** Human hepatocellular carcinoma cells (HepG2) were obtained from ATCC (American Type Culture Collection, Rockville, MD). The cells were maintained in Dulbecco's modified Eagle's medium (DMEM, Gibco) supplemented with 10% fetal bovine serum (FBS, Hyclone, Logan, UT), streptomycin at 100 µg/mL, penicillin at 100 U/mL, and 4 mM L-GLUTAMINE AT 37 °C IN A HUMIDIFIED 5% CO<sub>2</sub>-CONTAINING ATMOSPHERE.

Cytotoxicities of CS with molecular weight 200 kDa, empty CS-PAA nanospheres, free DOX, and CS-PAA-DOX nanospheres were evaluated using MTT assay.<sup>25</sup> The cell viability was determined by a microplate reader (GENios). Cells were transferred to 96-well plate first to ensure  $1 \times 10^4$  cells per well. Medium was changed every other day until 80% confluence was reached. Then, the medium was changed with 100 µL medium containing CS, CS-PAA nanospheres, free DOX, or CS-PAA-DOX nanospheres with various concentrations (for CS, we added little acidic acid to the medium to ensure that CS was soluble in the medium). One row of the 96-well plates was used as control. After 4-h incubation, the medium in each well was removed and the wells were washed three times using PBS. Ten microliters of 3-(4,5-dimethylthiazol-2-yl)-2,5-diphenyltetrazolium bromide (MTT) assay and 90 µL of medium were then added to the wells. After incubation for around 4 h, solution was removed, leaving the precipitate. One hundred microliters of isopropanol or DMSO was then added to the wells before the plate was observed using microplate reader. Cell viability was

determined by the following equation.

$$\text{cell viability \%} = \frac{I_{\text{sample}}}{I_{\text{control}}} \times 100\%$$

where  $I_{\text{sample}}$  and  $I_{\text{control}}$  represent the magnitude of intensity determined for cells treated with different samples and for control cells (nontreated), respectively.

**Drug Delivery in Vivo.** C57BL/6J mice, body weight between 18 and 22 g (provided by Central Animal Laboratory of China Pharmaceutical University), were used for in vivo. The mice were fasted overnight but had free access to water. Two hundred microliters of aqueous solution of CS-PAA-DOX nanospheres (corresponding to 100 mg nanospheres/kg body weight and 4.3 mg DOX per kg body weight) was injected intravenously (iv) into the tail vein. Three mice were iv injected with CS-PAA-DOX nanospheres or free DOX (4.3 mg per kg body weight) for each sampling point. At the predetermined time, blood samples were collected from the ocular artery after eyeball removal and were placed into heparinized test tubes. The animals were dissected and each objective organ was removed. The objective organs were washed with saline solution and were accurately weighed, homogenized, and stored at  $-80^{\circ}\text{C}$  till analysis. The study protocol was reviewed and approved by the Institutional of Animal Care and Use Committee, Nanjing University, P. R. China.

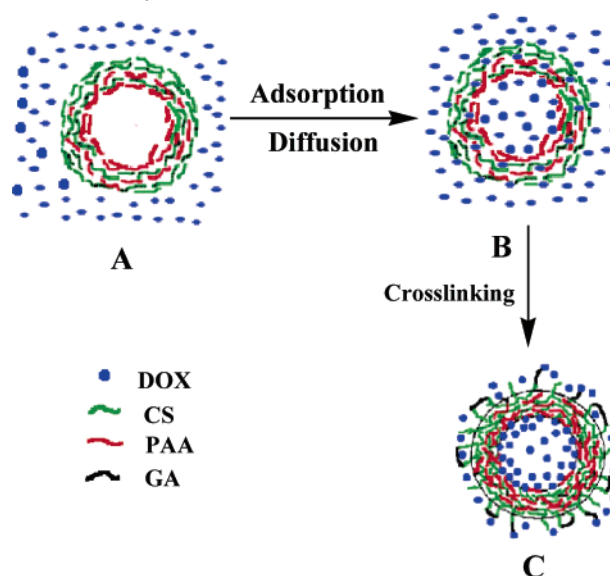
The concentration of DOX was assayed on a Shimadzu LC-10AD (Shimadzu, Japan) HPLC system using a Lichrospher C-18,  $5\mu$ , 200 cm  $\times$  4.6 mm RP-HPLC analytical column. The mobile phase consisted of 95/5 methanol (spectral grade, Merck, Germany)/double-distilled water (pH 5, adjusted with acetic acid). The column was eluted at a flow rate of 1.0 mL/min at  $30^{\circ}\text{C}$ . A Shimadzu RF-530 fluorescence detector (Shimadzu, Japan) was used to monitor the eluent. An excitation wavelength of 490 nm and an emission wavelength of 520 nm were applied in the quantification of DOX on the basis of the peak area with reference to a calibration curve. The blood samples and homogenized tissues were dissolved in PBS at pH 7.4 for 24 h on dark condition. Then, these samples were centrifuged at 12 000 rpm for 20 min at  $4^{\circ}\text{C}$ . The resulting supernatant was diluted to 5 mL by methanol. Twenty microliters of the clear mixed solution was injected into the HPLC system. The retention time of DOX was 3.04 min and the detection limit was 1 ng/mL. The recovery of pure DOX in all homogenized tissue samples was above 80%. Both intraday and interday variability was less than 5%.

**Confocal Laser Scanning Microscopy (CLSM).** C57BL/6J mice, body weight between 18 and 22 g (provided by Central Animal Laboratory of China Pharmaceutical University), were used for studies. Two hundred microliters of FITC-labeled CS-PAA nanospheres (corresponding to 100 mg nanospheres/kg body weight) was injected intravenously into the tail vein of mice. Three mice were iv injected with labeled CS-PAA nanospheres and the other three mice were injected with saline as the controls. Four hours after injection, animals were sacrificed by cervical dislocation. The brain and liver and other organs were removed, washed by saline, and frozen in Jung tissue freezing medium. After 24 h, these samples were cut into thin sections no more than 10  $\mu\text{m}$  with a microtomy at  $-24^{\circ}\text{C}$  (Leica CM 1900 Rapid Sectioning Cryostat, United States). These samples were viewed with a Bio-Rad MRC 1024 confocal laser scanning microscopy at  $\lambda_{\text{ex}} = 490\text{ nm}$  and  $\lambda_{\text{em}} = 520\text{ nm}$  (CLSM).

## Results and Discussion

**Preparation of CS-PAA-DOX.** In a previous work,<sup>18</sup> we have demonstrated that the CS-PAA hollow nanospheres could be prepared by polymerization of acrylic acid monomers in the presence of chitosan, followed by selective cross-linking of chitosan using GA. The hollow structure of these nanospheres was observed from the cut-section image of transmission electron microscopy (TEM) by microtomy at room temperature

**Scheme 1.** The Schematic Illustration of DOX Encapsulation into CS-PAA Nanospheres



of specimens embedded in epoxy resin. It was progressively found that the CS-PAA hollow nanospheres were composed of an outer shell of protonated CS chains and an inner shell of CS-PAA polyelectrolyte complex. This CS-PAA polyelectrolyte complex inner shell seems to be very compact and prevents macromolecules such as CS to penetrate into the core to further complex with PAA molecules. However, for small molecules, such as DOX, it can go through this layer easily. Furthermore, as reported by Kitaeva et al., since DOX molecule contains an amino group with a pKa of 8.6, and PAA contains carboxyl groups with a pKa of 4.8, DOX can form polyelectrolyte complex with the PAA chains.<sup>26</sup> On the basis of these results, we think that DOX can be encapsulated into hollow CS-PAA nanospheres by the interaction between DOX and PAA.

The encapsulation procedure of DOX into CS-PAA nanospheres is schematically illustrated in Scheme 1. When doxorubicin (DOX) was just added into the non-cross-linked CS-PAA nanosphere solution, there was no doxorubicin inside the CS-PAA nanospheres as shown in Scheme 1A. However, because the concentration of DOX was higher outside the CS-PAA nanospheres than that of inside the CS-PAA nanospheres, the DOX molecules will diffuse from the high concentration to low concentration. Thus, the DOX molecules would surround the nanospheres and move into the interior of nanospheres because of the diffusion effect (Scheme 1B). These DOX molecules inside nanosphere would interact with PAA to form PAA-DOX complex. This interaction caused more and more DOX molecules to penetrate into the CS-PAA nanospheres and to form the PAA-DOX complex continuously. As a result, DOX was encapsulated in the nanospheres (Scheme 1B). After crosslinking, the CS shell became more compact, which restricted the encapsulated DOX molecules going out of the nanospheres freely. Meanwhile, some DOX molecules may be conjugated onto the surface of CS-PAA nanospheres because of the cross-linking reaction between aldehyde group and amine group (Scheme 1C).

Figure 1 represents the FT-IR spectra of DOX, non-cross-linked CS-PAA nanospheres, DOX loaded non-cross-linked CS-PAA nanospheres, and CS-PAA-DOX nanospheres. Comparing the spectrum of non-cross-linked CS-PAA nanospheres with that of DOX loaded non-cross-linked CS-PAA nanospheres, it can be seen that the peak at  $1630\text{ cm}^{-1}$  appears significantly in the



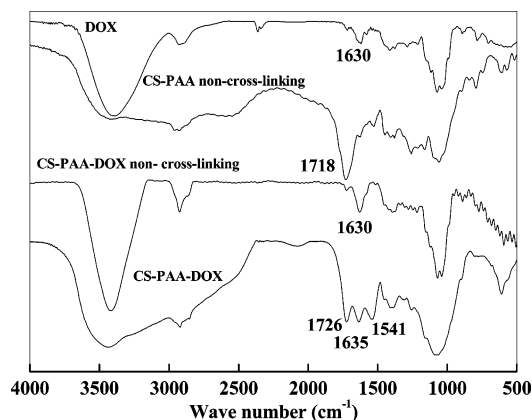


**Figure 1.** FT-IR spectra of DOX, non-cross-linked CS-PAA nanospheres, DOX loaded non-cross-linked CS-PAA nanospheres, and CS-PAA-DOX nanospheres.

DOX encapsulated non-cross-linked CS-PAA nanospheres. This peak is attributed to the vibration of hydroxyl group of hydroxybenzene structure in the DOX and can be seen in the pure DOX spectrum. This result indicates that DOX is encapsulated in the CS-PAA nanospheres. After cross-linking, a new peak at  $1635\text{ cm}^{-1}$  appears in the spectrum of CS-PAA-DOX nanospheres, which can be assigned to group of  $\text{C}=\text{N}$ , yielded by the cross-linking reaction.<sup>27</sup> In addition, after DOX is loaded, the peaks at  $3400\text{ cm}^{-1}$  (the absorption band of OH) and  $1065\text{ cm}^{-1}$  (glucosidic ring vibration), which show strong absorption in pure DOX spectrum, become more significant than that of drug-free sample. These results indicate that DOX is indeed loaded into CS-PAA hollow nanospheres.

**Size Distribution.** The size and size distribution of CS-PAA and CS-PAA-DOX hollow nanospheres in aqueous medium were characterized by DLS, and the results are represented in Figure 2. From Figure 2A, a unimodal size distribution with the polydispersity index of  $0.107 \pm 0.015$  for CS-PAA hollow nanospheres is observed, suggesting that the size distribution of synthesized CS-PAA hollow nanospheres is narrow before DOX was added. The mean size of CS-PAA nanospheres in aqueous solution was determined to be  $114.5\text{ nm}$ . On the other hand, after DOX was loaded, the size of nanospheres became  $118.0\text{ nm}$ , which is slightly larger than CS-PAA nanospheres. Furthermore, a bimodal size distribution of the CS-PAA-DOX nanospheres with a dominant peak at about  $100\text{ nm}$  and a minor peak around  $450\text{ nm}$  is observed, suggesting that a few bits of cross-linking reaction take place between nanospheres. In addition, zeta potential measurement showed that both CS-PAA nanospheres and CS-PAA-DOX nanospheres had a positive zeta potential (about  $20\text{ mV}$ ), indicating that the nanospheres possess a positively charged surface.

**DOX Release Behavior in Vitro.** Figure 3 shows the release profiles of DOX from CS-PAA-DOX nanospheres and non-cross-linked CS-PAA nanospheres at saline solution. The inset shows the initial release stage to illustrate the initial burst release. The DOX encapsulation efficiencies are  $68.9\%$  and  $59.2\%$  and DOX loading content is  $4.3\%$  and  $3.7\%$  for CS-PAA-DOX nanospheres and non-cross-linked CS-PAA nanospheres, respectively. These values are higher than those of nanoparticles consisting of DOX-PLGA conjugate<sup>28</sup> and indicate that the cross-linking process causes a slight increase in the DOX loading efficiency and loading content.

From Figure 3, it can be seen that in-vitro DOX release from CS-PAA-DOX nanospheres shows a very small initial burst. Only  $20\%$  DOX is released in the first  $5\text{ h}$ , which is much smaller than that of the non-cross-linked CS-PAA nanospheres

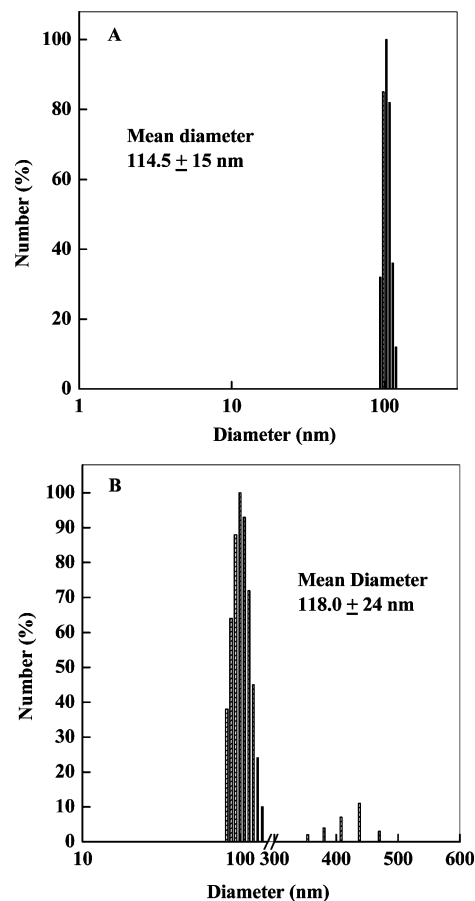


**Figure 2.** Size distribution of CS-PAA (A) and CS-PAA-DOX (B) hollow nanospheres in aqueous medium. (A break represents a cut in the range from  $150$  to  $300\text{ nm}$  since no nanosphere existed in this range.)

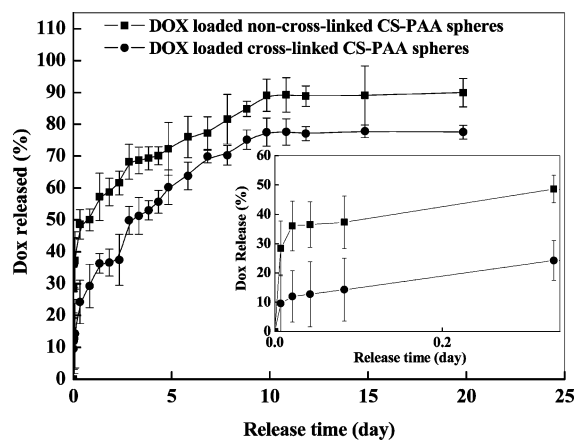


**Figure 3.** In-vitro release behavior of DOX from non-cross-linked CS-PAA nanospheres and CS-PAA-DOX nanospheres in saline solution at  $37\text{ }^{\circ}\text{C}$ .

(about  $45\%$ ). These differences in drug-loading efficiency, drug-loading content, and drug release can be ascribed to the CS shell cross-linking. The CS-PAA-DOX nanospheres have a more compact shell compared with that of non-cross-linked nanospheres, which restricts the diffusion of DOX from the interior of CS-PAA-DOX nanospheres and, in turn, enhances the drug-loading efficiency and content in nanospheres. After the initial burst stage, these two kinds of drug-loaded nanospheres provide a continuous release of the entrapped DOX up to  $10$  days and then reach a plate. Finally, about  $75\%$  and  $90\%$  encapsulated DOX are released from CS-PAA-DOX and non-cross-linked

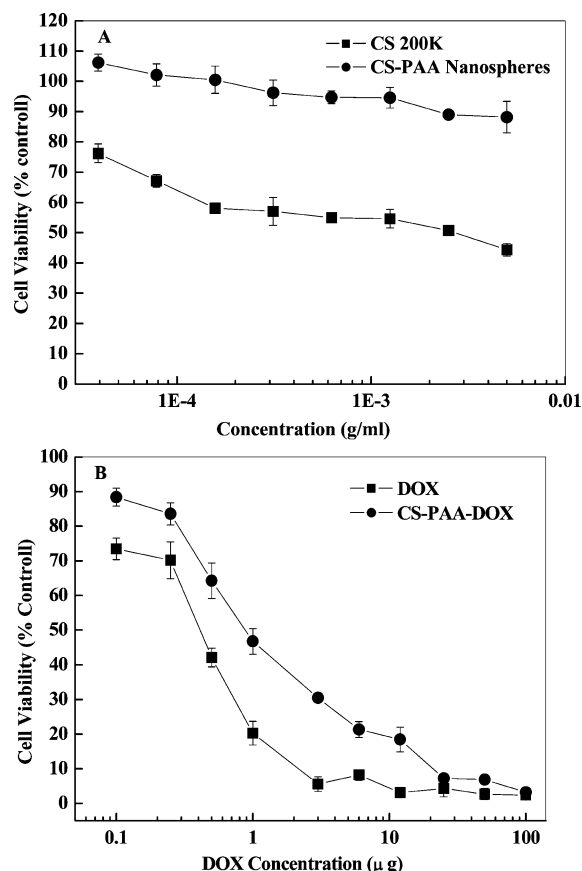


**Figure 4.** The cytotoxicity of CS 200K and empty CS-PAA nanospheres (A) and free DOX and CS-PAA-DOX nanospheres (B) in HepG2 cells. Data represent the mean value from  $n = 4$  and the standard error from the mean.

CS-PAA nanospheres, respectively. This result suggests that the CS-PAA-DOX nanospheres show a sustained release behavior for DOX.

**In-Vitro Cytotoxicity Effect.** The cytotoxicity effect of CS-PAA-DOX nanospheres was studied in vitro with cultured human hepatocellular carcinoma cells (HepG2). For comparison, the cytotoxicity of empty hollow nanospheres (CS-PAA), free DOX molecules, and CS with molecular weight of 200 kDa (CS 200K) was also evaluated. Figure 4 reveals the cytotoxicity of the objective materials in HepG2 cell line using the MTT assay.

From Figure 4A, it is found that empty CS-PAA nanospheres do not show the toxicity on the HepG2 cell line within the test concentration, even at the highest concentration tested, while CS molecules show the cytotoxicity in some extent, especially, in the higher concentration, which can be ascribed to too many positive charges in CS molecules and their interaction with negatively charged cell components and proteins.<sup>29</sup> This is supported by the measurements of the zeta potential of CS molecules (more than 60 mV) and CS-PAA nanospheres (about 20 mV). Figure 4B presents the cytotoxicity of free DOX and CS-PAA-DOX nanospheres. It can be seen that the cytotoxicity of CS-PAA-DOX is slightly lower than the free DOX in most tested concentrations except in higher DOX concentration. This can be attributed to the following reason: when free DOX and CS-PAA-DOX nanospheres were incubated with HepG2 cell line, free DOX was transport into cells by a passive diffusion mechanism, while CS-PAA-DOX nanospheres were captured by HepG2 cells by a possible endocytosis mechanism and the DOX molecules were gradually released, as shown in the in-vitro release profiles. Thus, in the cytotoxicity experiment,

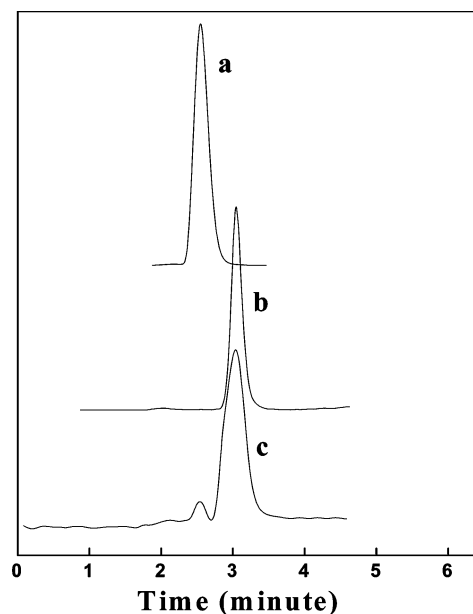


**Figure 5.** Typical chromatograms obtained during HPLC test in the in-vivo release study. (a) The extract of mouse liver homogenate; (b) The DOX ethanol solution (corresponding to 10 ng/mL); (c) The extract of the mouse liver homogenate with DOX solution.

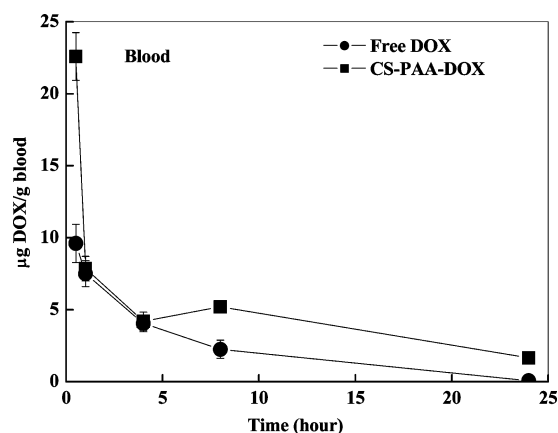


**Figure 6.** The DOX concentrations in plasma of mice over 24 h after injection ( $n = 3$ ).

although the CS-PAA-DOX nanospheres were incubated in cells for 4 h, it seems still to be insufficient to CS-PAA-DOX nanospheres to release DOX and reach enough DOX concentration causing the higher cytotoxicity than free DOX. This is in agreement with previous observation.<sup>28</sup>

**In-Vivo DOX Delivery.** To evaluate the drug delivery of CS-PAA-DOX nanospheres in vivo, we studied the concentration of DOX in different organs at different times after the CS-PAA-DOX nanospheres were injected into mice. Figure 5 shows the typical HPLC chromatograms obtained in the examination of DOX concentration in vivo. It can be seen that under the selected HPLC conditions, HPLC provides good separation between DOX and the lipophilic substances in tissue homogenates.

The DOX levels in plasma were determined following a single injection of CS-PAA-DOX (4.3 mg/kg DOX equiv) as described in the Experimental Section. The resulting DOX concentrations in plasma over 24 h at different time points (0.5, 1, 4, 8, 24 h) are given in Figure 6. The concentration of DOX in plasma is  $22.5 \pm 1.6 \mu\text{g/g}$  plasma) at half an hour following injection and decreases to  $1.7 \pm 0.25 \mu\text{g/g}$  plasma) after 24 h postinjection. As a comparison, DOX concentration is  $9.6 \pm 1.3 \mu\text{g/g}$

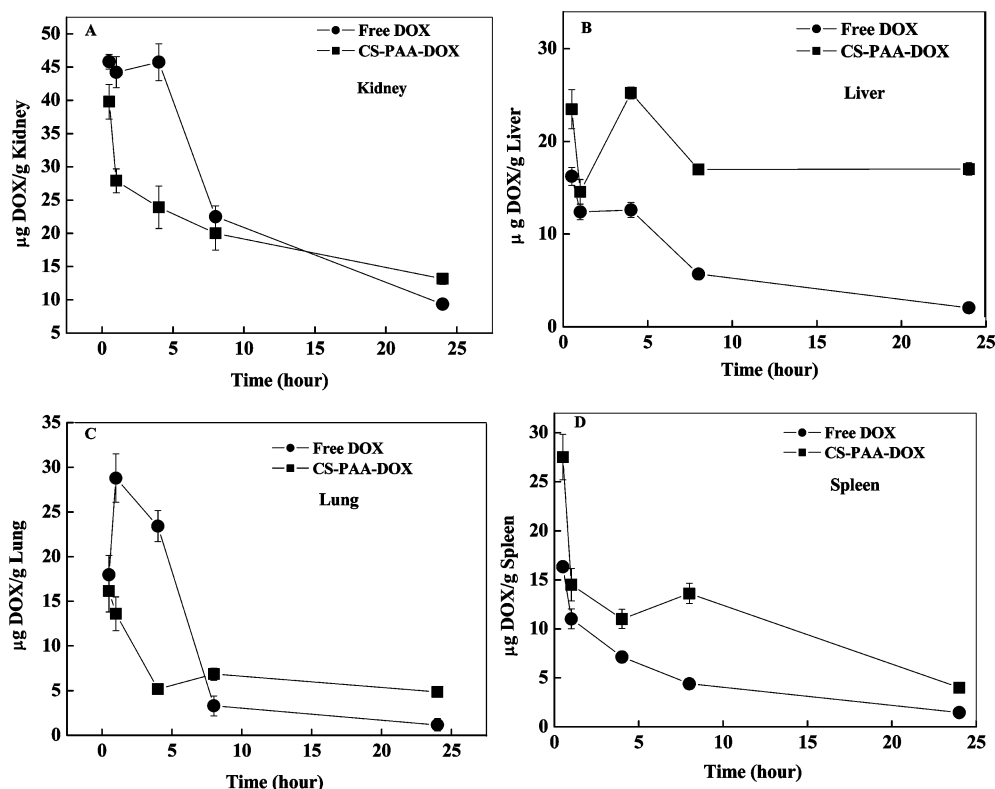


**Figure 7.** The concentration of DOX released from CS-PAA nanospheres in vivo in different organs at different times after injection.

(g plasma) at half an hour following injection and rapidly decreases to undetectable level after 24 h postinjection for free DOX solution. This phenomenon indicates that CS-PAA-DOX nanospheres prolong the circulation time of DOX in the blood, resulting in considerably high DOX concentration in blood than free DOX solution at extended time period.

Figure 7A, B, C and D shows the concentration of DOX in kidney, liver, lung, and spleen, respectively. For the kidney, spleen, and lung three organs, high initial concentrations of DOX are observed, and then DOX concentrations decay fast for both CS-PAA-DOX nanospheres and free DOX solution. In addition, a lower DOX concentration in kidney and lung for CS-PAA-DOX nanospheres than for free DOX solution in the initial administration time is observed. For liver, the difference in drug concentration between CS-PAA-DOX nanospheres and free DOX solution is obvious. When free DOX solution was injected in mice, the DOX concentration in liver decayed fast and the concentration of DOX in liver is below  $4 \mu\text{g}/(\text{g, liver})$  after 24 h. For the CS-PAA-DOX nanospheres, the concentration of DOX decayed in the first 8 h but then remains constant at about  $17 \mu\text{g}/(\text{g, liver})$  in the extended time period. The maximum in DOX concentration for CS-PAA-DOX nanospheres in liver is about  $25.3 \pm 0.65 \mu\text{g}/(\text{g, liver})$  at 4 h postinjection, which equals 33% of total injected DOX at time zero. These results indicate that CS-PAA nanospheres can alter the DOX biodistribution in animal. DOX mainly concentrates in liver, and its amount remains at a relatively high level during the whole testing time period. The most likely reason is that CS-PAA nanospheres are mechanically filtered by the liver, which makes them passively target the liver and may be useful in the treatment of liver cancer.

It is also interesting to examine whether the CS-PAA hollow nanospheres can carry DOX to the brain. Figure 8 gives the DOX concentration in the brain at different time intervals after injection. In contrast to free DOX solution, we detected DOX in the brain even after 24 h when CS-PAA-DOX nanospheres were injected into the mice. The DOX concentration decays

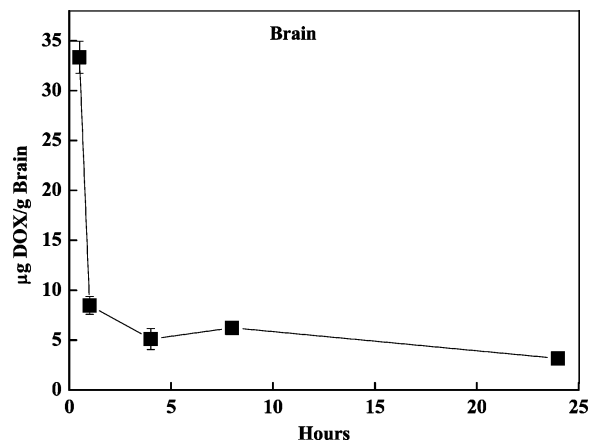


**Figure 8.** The DOX concentration in brain at different times after injecting CS-PAA-DOX nanospheres.

very fast during the first 1 h. It is about  $33 \mu\text{g}/(\text{g, brain})$  at half an hour and decreases to  $8 \mu\text{g}/(\text{g, brain})$  after 1 h. After then, the concentration is maintained at about  $5 \mu\text{g/g}$  even after 24 h. On the other hand, free DOX molecules are not able to be detected even at the initial time after injection. This result indicates that these hollow CS-PAA-DOX nanospheres are able to deliver DOX to the brain of mice.

To provide further evidence for CS-PAA nanospheres in mouse bodies, we used FITC labeled CS-PAA nanospheres to study their distribution in different tissues of mice with the aid of confocal laser scanning microscopy. Figure 9 shows the CLSM images of FITC labeled CS-PAA nanospheres in brain, liver, and spleen 4 h postinjection. It is clear that there are weak fluorescence signals (spots) in the brain (Figure 9A) and strong fluorescence signals (spots) in the mouse liver and spleen (Figure 9B and C). For the control (saline), there is no fluorescence signal (spots) in liver, spleen, and brain (images are not shown).

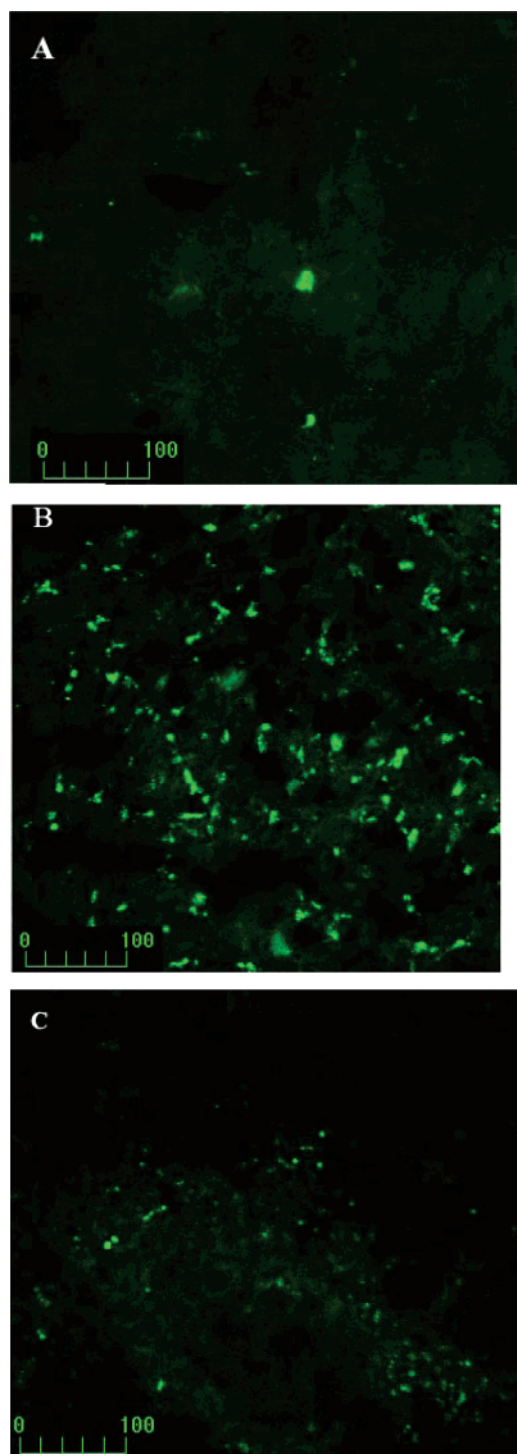


**Figure 9.** The CLSM images of FITC-labeled CS-PAA nanospheres in mice 4 h postinjection. (A) brain; (B) liver; (C) spleen.

These results further demonstrate that CS-PAA nanospheres can deposit in different organs and carry DOX to liver, spleen, and brain.

It has been reported that polysorbate 80-coated poly(butylcyanoacrylate) nanoparticles could cross the blood brain barriers (BBB) and deliver drugs to the brain because of the strong interaction between polysorbate 80 and brain microvessel endothelial cells.<sup>30</sup> In our case, the good mucoadhesive properties of both chitosan and PAA may enhance the interaction between the CS-PAA nanospheres and brain microvessel endothelial cells, resulting in the transfer ability of CS-PAA nanospheres to the brain. However, to address this transfer

ability and to demonstrate if the CS-PAA hollow nanospheres can cross BBB, more experimental evidence is needed and investigation of these issues will be the subject of forthcoming work.

## Conclusions

The preparation, in-vitro release, in-vitro cytotoxicity, and in-vivo drug delivery of DOX-loaded CS-PAA hollow nanospheres were investigated. DOX can be encapsulated in these hollow nanospheres and released in a sustained manner with low initial burst release. The in-vitro cytotoxicity of DOX-loaded CS-PAA hollow nanospheres is comparable to the free DOX. In-vivo release results reveal that CS-PAA nanoparticles can alter the DOX delivery in different organs of mouse body and show more effective drug delivery in liver and brain. Confocal laser scanning microscopy results confirm that these hollow nanospheres can be deposited in liver, spleen, and brain, indicating that the hollow CS-PAA nanospheres have promising potential as carriers for drugs.

**Acknowledgment.** This work is supported by the Natural Science Foundation of China (No.20374026, No.50625311, 50573031, No.50603008, No.10334020) and by the 973 Program of MOST (No.2003CB615600).

## References and Notes

- (1) Gref, R.; Minamitake, Y.; Peracchia, M. T.; Trebetskoy, V. S.; Torchilin, V. P.; Langer, R. *Science* **1994**, *263*, 1600–1603.
- (2) Yasugi, K.; Nagasaki, Y.; Kato, M.; Kataoka, K. *J. Controlled Release* **1999**, *62*, 89–100.
- (3) Hu, Y.; Jiang, X.; Ding, Y.; Zhang, L.; Yang, C. Z.; Zhang, J.; Chen, J.; Yang, Y. *Biomaterials* **2003**, *24*, 2395–2404.
- (4) Kwon, G. S.; Okano, T. *Adv. Drug Delivery Rev.* **1996**, *21*, 107–116.
- (5) Moghimi, S. M.; Hunter, A. C.; Murray, J. C. *Pharmacol. Rev.* **2001**, *53*, 283–318.
- (6) Hu, Y.; Zhang, L. Y.; Cao, Y.; Jiang, X. Q. *Biomacromolecules* **2004**, *5*, 1756–1762.
- (7) Nobs, L.; Buchegger, F.; Gurny, R. *J. Pharm. Sci.* **2004**, *93*, 1980–1992.
- (8) Barratt, G. *Cell. Mol. Life Sci.* **2003**, *60*, 21–37.
- (9) Caruso, F.; Caruso, R. A.; Mohwald, H. *Science* **1998**, *282*, 1111–1114.
- (10) Sauer, M.; Meier, W. *Chem. Commun.* **2001**, *01*, 55–56.
- (11) Dou, H. J.; Jiang, M.; Peng, H. S. *Angew. Chem., Int. Ed.* **2003**, *42*, 1516–1519.
- (12) Mao, H. Q.; Roy, K.; Troung-Le, V. L.; Leong, K. M. *J. Controlled Release* **2001**, *70*, 399–421.
- (13) Calvo, P.; RemunanLopez, C.; VilaJato, J. L. *J. Appl. Polym. Sci.* **1997**, *63*, 125–132.
- (14) Schatz, C.; Domard, A.; Viton, C. *Biomacromolecules* **2004**, *5*, 1882–1892.
- (15) Douglas, K. L.; Tabrizian, M. *J. Biomater. Sci., Polym. Ed.* **2005**, *16*, 43–56.
- (16) Ding, Y.; Hu, Y.; Jiang, X. Q. *Angew. Chem., Int. Ed.* **2004**, *43*, 6369–6372.
- (17) Hu, Y.; Jiang, X. Q.; Ding, Y. *Biomaterials* **2002**, *23*, 3193–3201.
- (18) Hu, Y.; Jiang, X. Q.; Ding, Y. *Adv. Mater.* **2004**, *16*, 933–937.
- (19) Young, C.; Ozols, R. F.; Myers, C. E. *New Engl. J. Med.* **1981**, *305*, 139–153.
- (20) Brigger, I.; Dubernet, C.; Couvreur, P. *Adv. Drug Delivery Rev.* **2002**, *54*, 631–651.
- (21) Bibby, D. C.; Talmadge, J. E.; Dalal, M. K. *Int. J. Pharm.* **2005**, *293*, 281–290.
- (22) Peer, D.; Margalit, R. *Neoplasia* **2004**, *6*, 343–353.
- (23) Qurashi, M. T.; Blair, H. S.; Allen, S. J. *J. Appl. Polym. Sci.* **1992**, *46*, 255–261.
- (24) Huang, M.; Ma, Z. S.; Khor, E.; Lim, L. Y. *Pharm. Res.* **2002**, *19*, 1488–1494.
- (25) Zhang, X. Q.; Wang, X. L.; Zhang, P. C.; Mao, H. Q.; Leong, K. M.; Zhuo, R. X. *J. Controlled Release* **2005**, *102*, 749–763.

- (26) Kitaeva, M. V.; Melik-Nubarov, N. S.; Menger, F. M. *Langmuir* **2004**, *20*, 6575–6579.
- (27) Oyrton, A. C.; Monteiro, J.; Claudio, A. *Int. J. Biol. Macromol.* **1999**, *26*, 119–128.
- (28) Yoo, H. S.; Lee, K. H.; Oh, J. E. *J. Controlled Release* **2000**, *68*, 419–431.
- (29) Fischer, D.; Li, Y.; Ahlemeyer, B.; Kriegelstein, J.; Kissel, T. *Biomaterials* **2003**, *24*, 1121–1131.
- (30) Gulyaev, A. E.; Gelperina, S. E.; Skidan, I. N. *Pharm. Res.* **1999**, *16*, 1564–1569.

BM0608176